J Nanostruct 13(3): 664-672, Summer 2023

RESEARCH PAPER

Comparison of Green and Chemical Synthesis of Tin Oxide Nanoparticles via Co-precipitation Technique and Analysis of Its Optical Properties

Merat Karimi [1], Mostafa Zahedifar [1,2], Ehsan Sadeghi [1,2], Bahareh Mohammadzadeh [1]*

[1] *Institute of Nano science and nanotechnology, University of Kashan, Kashan, Iran*

[2] *Department of Physics, University of Kashan, Kashan, Iran*

ARTICLE INFO

Article History:
Received 19 March 2023
Accepted 27 May 2023
Published 01 July 2023

Keywords:
Antibacterial
Green chemistry
Nanoparticles
Surfactant
Tin oxide

ABSTRACT

In this research two methods were used for the co-precipitation synthesis of tin oxide NPs, the first was by the chemical synthesis using the CTAB surfactant and the second was the green synthesis employing Teucrium polium plant as the surfactant. The structure of the NPs was identified by the X-ray diffraction pattern (XRD). Also, the scanning electron microscopy (SEM) was utilized to recognition of morphology of the NPs. And for determining the functional groups of the particles, Fourier-transform infrared spectroscopy (FTIR) was applied and photoluminescence spectroscopy (PL) was used for the analysis of the optical properties of the NPs. Debye Scherer formula was used to estimate the average size of the crystallites which was evaluated about 10nm and 17nm for the green and chemical synthesis respectively. The SEM images revealed that the size of the NPs for the green synthesis was 15-20nm and for the chemical synthesis the NPs, the size was approximately 20-30nm. The FTIR spectra confirmed the existence of the functional groups expected for the both methods. The maximum intensity in Pl profile appeared at wavelength around 398nm both for the green and chemical syntheses. Antibacterial analysis showed that they had a huge impact on pathogenic bacterial species. The minimum inhibitory concentrations of tin oxide NPs (MIC) for standard strains of Staphylococcus aureus ATCC 43300 and Pseudomonas aeruginosa PAO1 are 13.16±0.28µg/ml and 6.41±0.38 C, respectively.

How to cite this article
Karimi M., Zahedifar M., Sadeghi E., Mohammadzadeh B. Comparison of Green and Chemical Synthesis of Tin Oxide Nanoparticles via Co-precipitation Technique and Analysis of Its Optical Properties. J Nanostruct, 2023; 13(3):664-672. DOI: 10.22052/JNS.2023.03.007

INTRODUCTION

Nanotechnology is one of the most important achievements of the latest century which plays a key role in bond physics, chemistry, biology, and metallurgy together[1]. When components are brought to nanoscale, the way they operate changes and a lot of their physical properties changes[2]. The metal oxide structures that have an extensive bandgap are of importance as semi-conductors in chemistry and physics [3] and because of the important properties of metal oxides in nanoscale such as optical, electrical, magnetic, and structural properties, they have different applications in sensors, catalyzers, and photocatalysts, micro-electronics. nonlinear optics, photoelectrochemistry, imaging science,

* *Corresponding Author Email: zhdfr@kashanu.ac.ir*

and electro-optical science[4-6]. Tin(IV)oxide (SnO_2) is one of the important nanostructures that has been given a lot of attention due to its transparency in the visible wavelength spectrum and other properties such as high carrier density, high-temperature tolerance, chemical stability, and low resistivity[4, 7]. SnO_2 is an n-type semiconductor with a bandgap of 3.6 eV[8].

In a study conducted by Boucherka Teldja et al., the effects of the combination of indium with tin oxide on the structure, morphology, optical and electrical properties of the combination were analyzed via the sol gel method. They have reported that the combination of indium with tin oxide improves the optical transmission and decreases the electrical conduction due to indium naturalness. In that research, thin films with high transmission and low resistance were obtained[9]. Ariya Nachiar and co-authors have reported that if the copper NPs are synthesized with tin oxide NPs using the co-precipitation method, the copper causes a change in the structural and optical properties of tin oxide NPs and reduces the bandgap of tin oxide NPs[2]. SnO_2 have many applications in gas and solid-state sensors, lithium batteries, electro-optical tools, as catalysts for the oxidation of organic components, ceramic and transparent conductors, biomedical and nanoelectronics[1, 3, 6, 10, 11], supercapacitors[12], plasma screens, touch screens[13], special coating for energy-conserving "low-emissivity" windows[14] and the electrodes of the solar cells [15].

There are different methods for accomplishing a chemical and physical synthesis of SnO_2 such as co-precipitation, micro-emulation, sol-gel, and hydrothermal methods [8, 16], RF magnetron sputtering[17], spray pyrolysis[18], chemical vapor deposition [19] and deposition via laser[15]. Also, the strong light emission of tin oxide and other metal semi-conductors have important applications in remote communication and driving signs[20].

The manufacture of NPs in different shapes and sizes is more biologically and chemically active due to the fact that the number of surface atoms increases to volumetric atoms and causes antimicrobial agents. NPs can invade and disrupt bacteria in a variety of ways. NPs bind to the bacterial membrane by electrostatic reaction or by reacting with amines and carboxyl groups of the peptidoglycan layer of the bacterial wall, disrupting it and destroying the cell walls, completely destroying the bacterium [21-23]. Studies have been performed on the antibacterial properties of tin oxide NPs. According to the results of this work, tin oxide NPs synthesized by chemical methods show good antibacterial properties[24]. Kamaraj et al. synthesized tin (IV) oxide nanoparticles in a green method using the methanolic extract of Cleistanthus Collinus plant and investigated their biological activities. They investigated the antibacterial activity of the synthesized nanoparticles against Escherichia coli and Staphylococcus aureus bacteria. Antifungal activity of nanoparticles was also investigated. In this research, the average size of the synthesized nanoparticles was reported to be 49.26 nm, the synthesized nanoparticles showed significant antibacterial activity against Escherichia coli [25]. Khan et al were also able to synthesize tin (IV) oxide nanoparticles through the green method and using the extract of Clerodendrum Inerme. They also investigated the antibacterial and anticancer activities of synthetic nanoparticles. Morphological and crystalline changes of synthesized nanoparticles were also investigated by XRD and TEM analyses [26]. Studies on the biosynthesis of nanoparticles in the extracts of different plants were very different and it was found that in different plants, the synthesized nanoparticles show different effects. Plant extracts have antioxidant properties and a lot of secondary compounds [27]. The average size of nanoparticles synthesized using Turicum puliom plant in this research is approximately 20 nm, which has a greater effect on bacteria compared to the previous studies.

The chemical methods for synthesizing the NPs are expensive and dangerous and the NPs produced with these procedures are highly toxic and hazardous to the environment. The green synthesizes of the NPs, using plants, is cheaper and non-toxic, these methods are ecofriendly and the components used in the synthesis procedure are easily found in the nature[10, 28]. Medicinal plants also have a biological state, so they do not accumulate in the body and do not cause side effects and therefore have a significant advantage over chemical drugs. Teucrium polium plant is known for its medicinal uses and has properties such as liver protector, antioxidant, anti-inflammatory, anti-tumor, and antibacterial and contains important compounds including diterpenoids, flavonoids, iridoids, sterols, and terpenoids[29, 30]. The

prevalence of drug-resistant microorganisms is a serious problem. Also, infections caused by these bacteria are leading causes of morbidity and mortality. Therefore, new research is needed for the development of antimicrobial compounds. One of the important antibacterial compounds is NPs. Herein, the Teucrium polium plant has been used for the first time to synthesize the tin oxide NPs using the co-precipitation method and the optical properties have been compared to the NPs produced with the chemical synthesis method. The procedure for producing the NPs with the green method was cheaper and was eco-friendlier than the one synthesized with the chemical method.

MATERIALS AND METHODS

The morphology and the size of NPs were identified using a Philips Scanning electron microscopy (SEM) of TESCAN-SEM Mira3-XMU. Fourier transform infrared spectroscopy (FTIR) model MagnaIR550 was employed to study the functional groups. The optical properties of the materials were investigated using the PerkinElmer LS55 photoluminescence spectrometer.

Preparation method

Teucrium polium plant extract was used as a surfactant for the green synthesis of tin oxide NPs. First, 1ml of the extract was added to 30ml of twice distilled water. Then, two drops of tin chloride was dissolved in 50ml of twice distilled water. After 30 minutes, the solution containing the extract of Teucrium polium was added to the tin solution and brown-colored sediment was obtained. The precipitate was removed using centrifugation and washed with water and ethanol. The precipitate was dried in an oven for 24 hours. The dried precipitate was placed in a furnace for a period of time to remove the excess components. For the chemical synthesis of NPs, two-aqueous tin chloride, ammonia and CTAB were used.

Determination of the minimum inhibitory concentration (MIC)

In this study, the antibacterial activity of the SnO_2 was evaluated against Staphylococcus aureus ATCC43300 and Psoudomonas aeroginosa PAO1.

Minimum inhibitory concentration (MIC) determine by the broth microdilution method, according to the Clinical and Laboratory Standards Institute (CLSI) guidelines. First, 100 µL of Mueller Hinton broths (MHB) loaded onto sterile 96-well plates. Afterward, dilution series of SnO_2 was prepared and added to the wells. Finally, 10 **µL** of bacterial suspension (5×10^5 CFU) was added to each well and then incubated at 37 °C for 24 h. The lowest concentration of NPs that inhibited the growth of bacteria was recorded as the minimum inhibitory concentration.

Antibiofilm Activity of SnO_2 against MRSA and PAO1 Biofilm

Microtiter plate (MTP) assay is a quantitative method to determine the Antibiofilm Activity of SnO_2. Bacterial suspension is 10-fold (1/10) diluted to reach 5.106 CFU/ml and 100 µl of bacterial suspensions are inoculated into 96-well flat-bottomed sterile polystyrene microplate in the absence and presence of, 1/8 MIC 1/4MIC, 1/2 MIC, and MIC concentrations of SnO_2. Wells involving biofilms were washed with phosphate-buffered saline (PBS). Then wells were fixed with methanol for 20 minutes. Subsequently, Biofilm mass was stained with 200 µL of 0.1% crystal violet for 15 minutes. Following the air-drying process of wells of a microplate, the dye of biofilms that lined the walls of the microplate is resolubilized by 200 µL glacial acetic acid. Then microplate is measured spectrophotometrically at 570 nm by a microplate reader.

$$\text{Percentage of biofilm inhibition} = \frac{\text{Control OD}-\text{Test OD}}{\text{Control OD}} \times 100$$

RESULT AND DISCUSSION

X-ray diffraction pattern (XRD)

XRD analysis was performed to determine the crystal structure and phase composition or phase purity of the sample. Fig. 1 shows the SnO_2 diffraction pattern at angles of 2θ=10-90 degrees which corresponds to the standard card number 1250-021-00 [31]. The observed peaks with the page numbers in 2θ=(002), (321), (202 (301), (310), (220), (211), (200), (101), (110) and confirms the diffraction pattern of nanoparticle synthesis which lattice structure is tetragonal [32]. The size of the crystals can be estimated from a maximum peak of the XRD spectrum.

The Scherer relation fairly shows the dependence of particle size on the amplitude and diffusion of diffraction lines:

$$D_{hkl} = \frac{k\lambda}{\beta\cos\theta}$$

In this respect, D is the approximate size of the

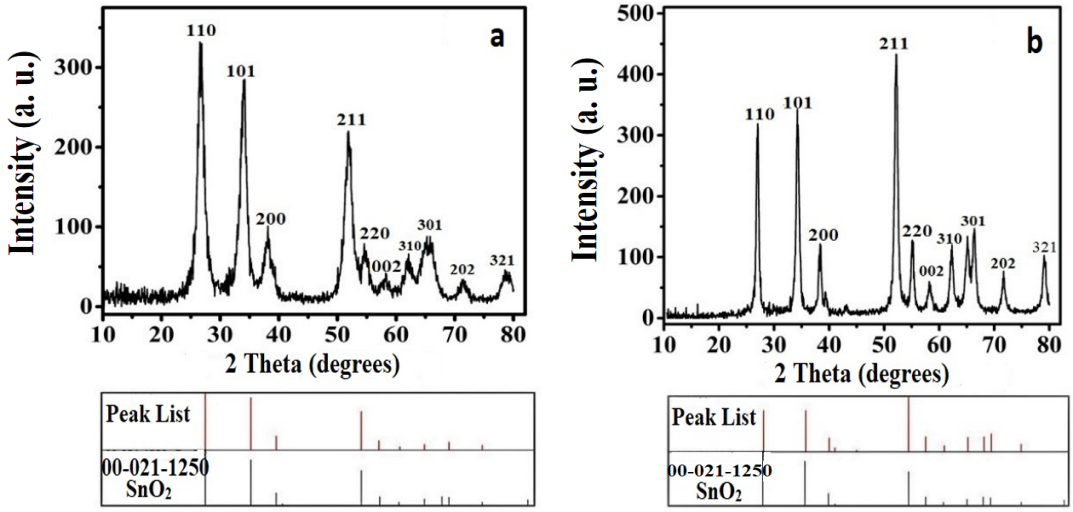

Fig. 1. XRD spectrum of green synthesis (a) and chemical synthesis (b) of tin dioxide NPs made by co-precipitation method.

crystallites, is the wavelength of the X-ray beam, and β is the full width at half maximum (FWHM) of the main peaks for the hkl plates and is the angle. Using the above relation, the size of tin oxide NPs for green and chemical synthesis was 10 nm and 17 nm, respectively. X-ray diffraction pattern analysis is the same for both green and chemical synthesis, except that the particle size in green synthesis is smaller, which can be detected by the enlargement of the peak.

X-ray energy diffraction spectroscopy (EDS) is a method that uses X-ray energy to analyze and determine the chemical composition of samples on a small scale [33]. Using the EDS spectrum, the phase purity of the NPs is obtained. The initial composition of the sample is shown in Fig. 2. According to this diagram, only SnO_2 existed and no additional impurities were observed.

Scanning electron microscope (SEM)

The SEM image of SnO_2 samples synthesized by co-precipitation is shown in Fig. 3. This image shows that the NPs are uniform and have spherical shape. Also, the size of NPs is in accordance with the size obtained from the Scherer formula. The size of the NPs obtained by the green synthesis (A) and chemical synthesis (B), obtained in the range of 15-20 nm and 20-30 nm, respectively according to the inset figures.

Photoluminescence Spectroscopy (PL)

One of the well-known types of luminescence is PL, in which excitation is done by photons. The process of excitation of electrons to a higher

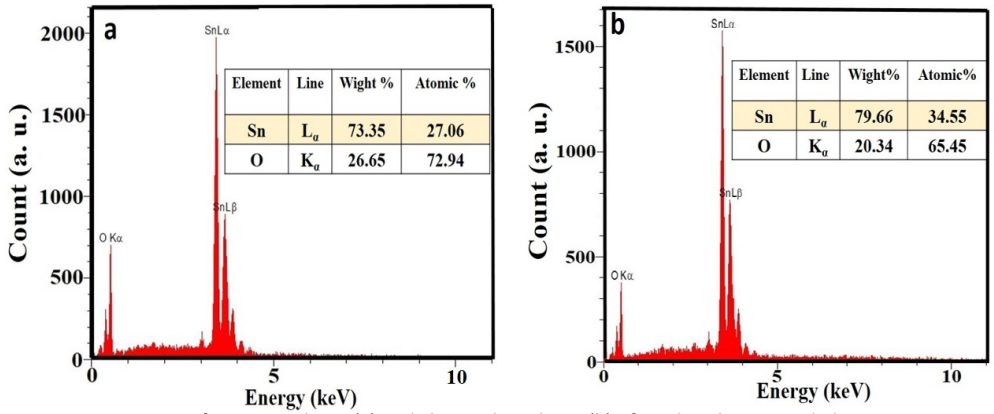

Fig. 2. EDX spectrum of green synthesis (a) and chemical synthesis (b) of tin dioxide NPs made by co-precipitation method.

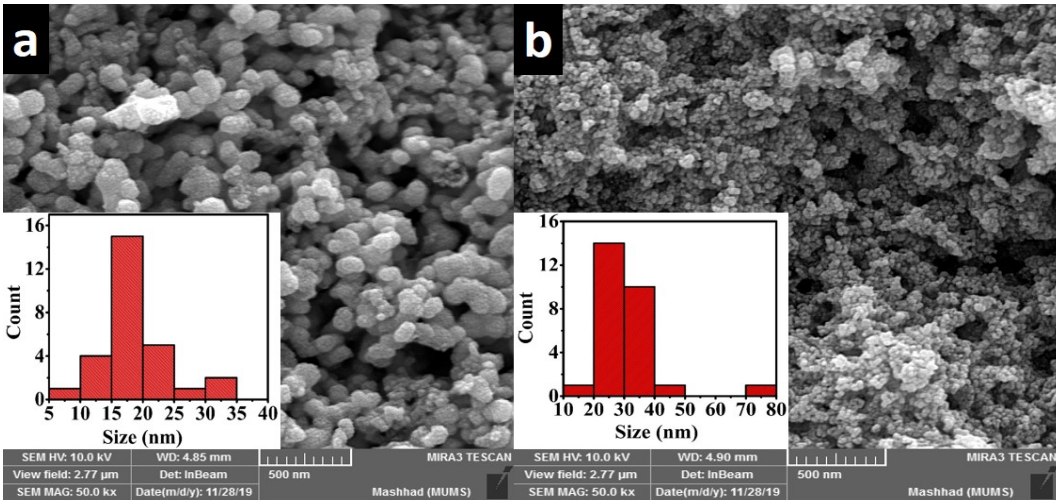

Fig. 3. SEM image of green synthesis (a) and chemical synthesis (b) of tin dioxide NPs made by co-precipitation method.

energy level and then their transition to a lower energy level is accompanied by the absorption and emission of photons. In the PL process, the sample is excited by a laser or a lamp and the spectrum is obtained by recording the emission as a function of wavelength. The study of PL is one of the important methods in studying the optical properties related to the adsorption and dispersion of nanomaterials, determining the optical quality, electronic structure, and photochemical properties of semiconductor materials and investigating the structure and properties of sites active on metal oxides and zeolites [34, 35]. In addition, PL can be used to study Crystal defects[36] and in the field of photocatalytic semiconductors, it is useful for understanding surface processes[37]. In nanostructured metal oxides, PL emission is divided into two main parts, including emission in the ultraviolet (UV) region and emission in the visible region. Emission in the UV region is associated with direct decay (band-band PL). Also, the emission in the visible region is the result of the radiative recombination of a hole with electrons in the oxygen and metal voids (excitonic PL) [38]. In semiconductor NPs, the sign of excitonic PL occurs, but the band-band PL signal is rarely observed [37] High emission intensity in the visible area is related to high concentrations of impurities and crystalline defects[39]. Defects such as oxygen voids are one of the most important and common defects in nanocrystalline oxides and act as luminous centers in the luminescence process[40]. The PL emission spectrum of tin oxide NPs in Fig. 4 was accomplished with the two methods mentioned,

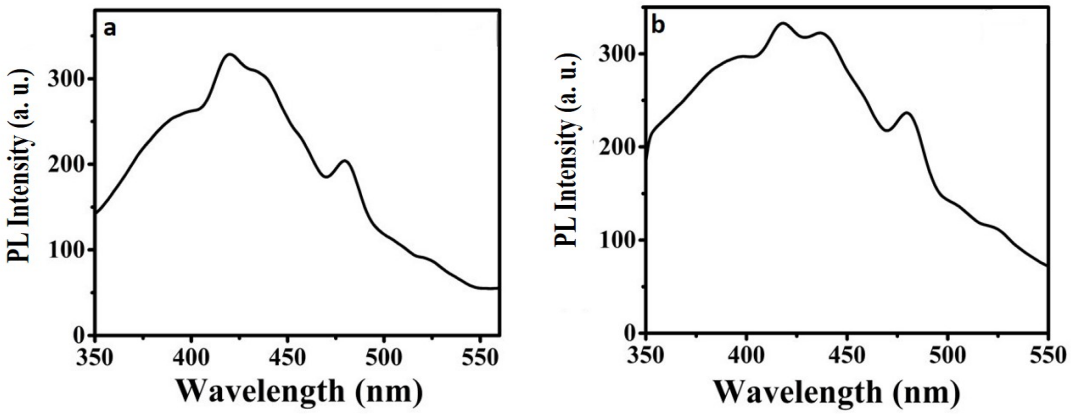

Fig. 4. Photoluminescence (PL) spectra of green synthesis (a) and chemical synthesis (b) of tin dioxide NPs excited at 280 nm.

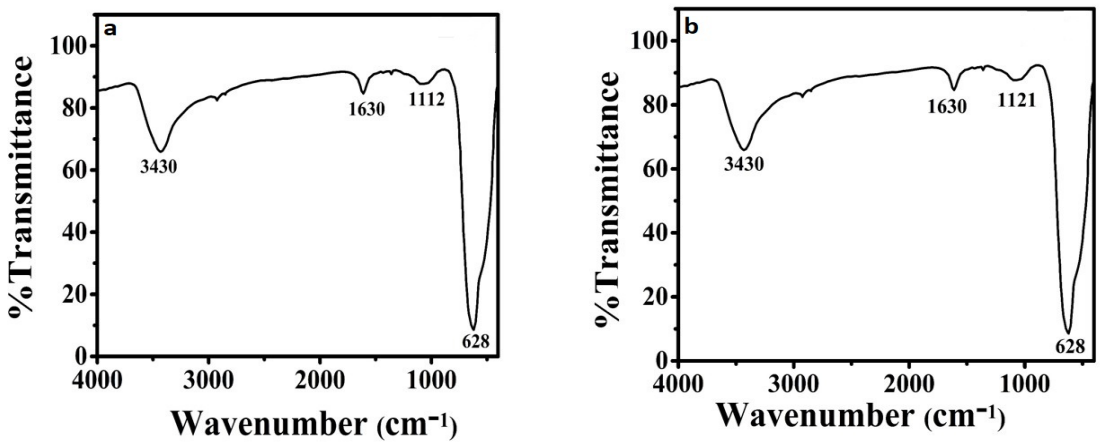

Fig. 5. FTIR spectrum of green synthesis (a) and chemical synthesis (b) of tin dioxide NPs made by co-precipitation method.

under excitation at the wavelength of 280nm, at room temperature, indicating that the maximum PL peak was about 398 nm for both syntheses.

Fourier Transform Infrared Spectroscopy

Infrared spectroscopy is a well-known technique in the qualitative identification of materials and is a method in which the absorption of radiation and vibrational mutations of molecules and ions of polyatoms are examined. This method is used as a powerful and developed technique for measuring chemical species and is mainly used to identify organic compounds because the spectra of these compounds are usually complex and have a large number of maximum and minimum peaks that can be used for comparison. In both spectra of Fig. 5, the broad absorption band is at 3430 cm^{-1}, which is related to the tensile vibrations of the O-H bond caused by the water adsorbed on the SnO_2 surface[41]. The adsorption band at 11630 cm^{-1} corresponds to C = C groups or aromatic or tensile rings in the C = O carboxyl group [42]. The absorption bands shown in the 1200-400 cm-1 range are known as fingerprint bands, which are different for each material. The tensile bonds of Sn-O-Sn, O-Sn-O, and Sn-O are located in this fingerprint region. The presence of these functional groups can be considered as light centers at the nanoparticle levels.

Investigation of antibacterial properties of NPs
Determination of the Minimum Inhibitory Concentration (MIC) and MBC

According to the data shown in Table 2, among the tested bacteria maximum antibacterial activity were demonstrated against *Pseudomonas*

Table 1. Minimum inhibitory concentration of tin oxide NPs (MIC) for standard strain of staphylococcus aureus ATCC 43300 Pseudomonas aeruginosa PAO1.

Microorganism	Minimum-Maximum (µg/ml)	Mean ± SD
Staphylococcus aureus ATCC 43300	13-13.5	13.16±0.28
Pseudomonas aeruginosa PAO1	6-6.75	6.41±0.38

Table 2. Minimum bactericidal concentration (MBC) of tin oxide NPs for standard strain of staphylococcus aureus ATCC 43300.

Microorganism	Minimum-Maximum (µg/ml)	Mean ± SD
Staphylococcus aureus ATCC 43300	27-54	36±15
Pseudomonas aeruginosa PAO1	13.5-27	22.5±7.7

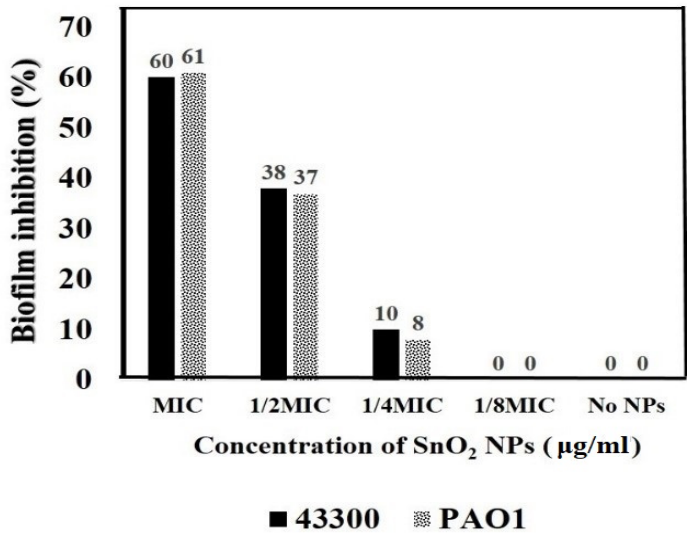

Fig.6. The effect of different concentrations of tin oxide NPs on the reduction of biofilm formation in the standard strain.

aeruginosa PAO1.

Staphylococcus aureus is one of the most common and important gram-positive bacteria in the hospital, which can range from skin infections to life-threatening diseases and is increasing nowadays [43, 44]. Pseudomonas aeruginosa is a gram-negative bacterium that is scattered all over the world and is one of the most important bacteria in hospital[45].

In an experiment of interaction between NPs and two bacteria, Pseudomonas aeruginosa PAO1 and Staphylococcus aureus ATCC 43300, with an average MIC and MBC of milligrams per milliliter, the NPs turned out to be capable of being used as drugs to remove bacterial strains, as shown in Tables 1 and 2.

Antibiofilm Activity of SnO_2 against MRSA and PAO1 Biofilm

SnO_2 NPs showed obvious inhibition of attachment and biofilm formation (Fig. 6). According to the result, the SnO_2 nanoparticle in concentration MIC of SnO_2 nanoparticle inhibited the biofilm formation by MRSA and PAO1 with an inhibition rate of 60% and 61% respectively. The effect of different concentrations of NPs on the reduction of biofilm formation in the standard strain of Staphylococcus aureus ATCC 43300 and the standard strain of Pseudomonas aeruginosa PAO1, each microplate used for two bacteria, and the nanoparticle for each stock bacterium was prepared with MIC concentration. The fractional concentration of NPs in sumps is 1/8 MIC, 1/4 MIC, and 1/2 MIC and zero. They were studied in the same way as shown in Fig. 6, with an increase in the percentage of formation error, Biofilm is reduced for two bacteria.

However, different studies may suggest that MIC may vary due to the size of the NPs and the preparation methods, as well as differences in the strains of the studied bacteria and that the effect of NPs on bacteria depends not only on cell wall structure but also on fat peroxidation and producing the active species of oxygen[46, 47].

CONCLUSION

Tin oxide NPs were synthesized by the co-precipitation method, using plants and chemicals as surfactants. The optical and antibacterial properties of SnO_2 NPs were investigated using SEM, PL, EDX, XRD, and FTIR methods. The results of both methods are the same. Due to the fact that the use of chemical methods causes great harm to human health and the environment, plant-based materials and green synthesis are essential for the production of NPs that are non-toxic and less hazardous for the environment. The antimicrobial results of tin oxide NPs in inhibiting the formation of bacterial biofilms can be used as a suitable solution in the use of NPs for microbial purification and environments that are more exposed to this bacterium.

CONFLICT OF INTEREST

The authors declare that there is no conflict of interests regarding the publication of this manuscript.

REFERENCE

1. Elango G, Kumaran SM, Kumar SS, Muthuraja S, Roopan SM. Green synthesis of SnO_2 nanoparticles and its photocatalytic activity of phenolsulfonphthalein dye. Spectrochimica Acta Part A: Molecular and Biomolecular Spectroscopy. 2015;145:176-180.
2. Nachiar RA, Muthukumaran S. Structural, photoluminescence and magnetic properties of Cu-doped SnO_2 nanoparticles co-doped with Co. Optics & Laser Technology. 2019;112:458-466.
3. Al-Saadi TM, Hussein BH, Hasan AB, Shehab AA. Study the Structural and Optical Properties of Cr doped SnO_2 Nanoparticles Synthesized by Sol-Gel Method. Energy Procedia. 2019;157:457-465.
4. Garrafa-Galvez HE, Nava O, Soto-Robles CA, Vilchis-Nestor AR, Castro-Beltrán A, Luque PA. Green synthesis of SnO_2 nanoparticle using Lycopersicon esculentum peel extract. J Mol Struct. 2019;1197:354-360.
5. Singh AK, Janotti A, Scheffler M, Van de Walle CG. Sources of Electrical Conductivity in SnO_2. Phys Rev Lett. 2008;101(5).
6. Safardoust-Hojaghan H. Rare earth–doped SnO_2 nanostructures and rare earth stannate ($Re_2Sn_2O_7$) ceramic nanomaterials. Advanced Rare Earth-Based Ceramic Nanomaterials: Elsevier; 2022. p. 231-258.
7. Zulfiqar, Khan R, Yuan Y, Iqbal Z, Yang J, Wang W, et al. Variation of structural, optical, dielectric and magnetic properties of SnO_2 nanoparticles. Journal of Materials Science: Materials in Electronics. 2016;28(6):4625-4636.
8. Luque PA, Nava O, Soto-Robles CA, Chinchillas-Chinchillas MJ, Garrafa-Galvez HE, Baez-Lopez YA, et al. Improved photocatalytic efficiency of SnO_2 nanoparticles through green synthesis. Optik. 2020;206:164299.
9. Teldja B, Noureddine B, Azzeddine B, Meriem T. Effect of indium doping on the UV photoluminescence emission, structural, electrical and optical properties of spin-coating deposited SnO_2 thin films. Optik. 2020;209:164586.
10. Jadhav DB, Kokate RD. Green synthesis of SnO_2 using green papaya leaves for nanoelectronics (LPG sensing) application. Materials Today: Proceedings. 2020;26:998-1004.
11. Matussin S, Harunsani MH, Tan AL, Khan MM. Plant-Extract-Mediated SnO_2 Nanoparticles: Synthesis and Applications. ACS Sustainable Chemistry & Engineering. 2020;8(8):3040-3054.
12. Liu Y, Jiao Y, Zhang Z, Qu F, Umar A, Wu X. Hierarchical SnO_2 Nanostructures Made of Intermingled Ultrathin Nanosheets for Environmental Remediation, Smart Gas Sensor, and Supercapacitor Applications. ACS Applied Materials & Interfaces. 2014;6(3):2174-2184.
13. Shin Y-H, Cho C-K, Kim H-K. Resistance and transparency tunable Ag-inserted transparent InZnO films for capacitive touch screen panels. Thin Solid Films. 2013;548:641-645.
14. Gu F, Wang SF, Lü MK, Zhou GJ, Xu D, Yuan DR. Photoluminescence Properties of SnO_2 Nanoparticles Synthesized by Sol–Gel Method. The Journal of Physical Chemistry B. 2004;108(24):8119-8123.
15. Wang X, Di Q, Wang X, Zhao H, Liang B, Yang J. Effect of oxygen vacancies on photoluminescence and electrical properties of (2 0 0) oriented fluorine-doped SnO_2 films. Materials Science and Engineering: B. 2019;250:114433.
16. Wei Q, Sun J, Song P, Yang Z, Wang Q. Synthesis of reduced graphene oxide/ SnO_2 nanosheets/Au nanoparticles ternary composites with enhanced formaldehyde sensing performance. Physica E: Low-dimensional Systems and Nanostructures. 2020;118:113953.
17. Ma J, Wang Y, Ji F, Yu X, Ma H. UV–violet photoluminescence emitted from SnO2:Sb thin films at different temperature. Mater Lett. 2005;59(17):2142-2145.
18. Abdelkrim A, Rahmane S, Abdelouahab O, Hafida A, Nabila K. Optoelectronic properties of SnO_2 thin films sprayed at different deposition times. Chinese Physics B. 2016;25(4):046801.
19. Yang JK, Zhao HL, Li J, Zhao LP, Chen JJ, Yu B. Structural and optical properties and photoluminescence mechanism of fluorine-doped SnO_2 films during the annealing process. Acta Mater. 2014;62:156-161.
20. Bhardwaj N, Satpati B, Mohapatra S. Plasmon-enhanced photoluminescence from SnO_2 nanostructures decorated with Au nanoparticles. Appl Surf Sci. 2020;504:144381.
21. Whitesides GM. Nanoscience, Nanotechnology, and Chemistry. Small. 2004;1(2):172-179.
22. Bogdanović U, Lazić V, Vodnik V, Budimir M, Marković Z, Dimitrijević S. Copper nanoparticles with high antimicrobial activity. Mater Lett. 2014;128:75-78.
23. Karimi M, Kashi MA, Montazer AH. Synthesis and characterization of ultrafine γ-Al_2O_3:Cr nanoparticles and their performance in antibacterial activity. J Sol-Gel Sci Technol. 2021;99(1):178-187.
24. Vidhu VK, Philip D. Biogenic synthesis of SnO_2 nanoparticles: Evaluation of antibacterial and antioxidant activities. Spectrochimica Acta Part A: Molecular and Biomolecular Spectroscopy. 2015;134:372-379.
25. Vennila R, Hasina Banu A, Kamaraj P, Devikala S, Arthanareeswari M, selvi JA, et al. A Novel Glucose Sensor Using Green Synthesized Ag Doped CeO_2 Nanoparticles. Materials Today: Proceedings. 2018;5(2):8683-8690.
26. Khan SA, Kanwal S, Rizwan K, Shahid S. Enhanced antimicrobial, antioxidant, in vivo antitumor and in vitro anticancer effects against breast cancer cell line by green synthesized un-doped SnO_2 and Co-doped SnO_2 nanoparticles from Clerodendrum inerme. Microb Pathog. 2018;125:366-384.
27. Gebreslassie YT, Gebretnsae HG. Green and Cost-Effective Synthesis of Tin Oxide Nanoparticles: A Review on the Synthesis Methodologies, Mechanism of Formation, and Their Potential Applications. Nanoscale research letters. 2021;16(1):97-97.
28. Sirohi K, Kumar S, Singh V, Chauhan N. Hydrothermal synthesis of Cd-doped SnO_2 Nanostructures and their Structural, Morphological and Optical Properties. Materials Today: Proceedings. 2020;21:1991-1998.
29. Rasekh HR, Khoshnood-Mansourkhani MJ, Kamalinejad M. Hypolipidemic effects of Teucrium polium in rats. Fitoterapia. 2001;72(8):937-939.
30. El-Shazly AM, Hussein KT. Chemical analysis and biological activities of the essential oil of Teucrium leucocladum Boiss. (Lamiaceae). Biochemical Systematics and Ecology. 2004;32(7):665-674.
31. Geng J, Ma C, Zhang D, Ning X. Facile and fast synthesis of SnO_2 quantum dots for high performance solid-state asymmetric supercapacitor. J Alloys Compd.

2020;825:153850.
32. Gong J-Y, Guo S-R, Qian H-S, Xu W-H, Yu S-H. A general approach for synthesis of a family of functional inorganic nanotubes using highly active carbonaceous nanofibres as templates. J Mater Chem. 2009;19(7):1037-1042.
33. Suvith VS, Devu VS, Philip D. Facile synthesis of SnO_2/NiO nano-composites: Structural, magnetic and catalytic properties. Ceram Int. 2020;46(1):786-794.
34. Anpo M, Tanahashi I, Kubokawa Y. Photoluminescence and photoreduction of vanadium pentoxide supported on porous Vycor glass. The Journal of Physical Chemistry. 1980;84(25):3440-3443.
35. Iwamoto M, Furukawa H, Matsukami K, Takenaka T, Kagawa S. Diffuse reflectance infrared and photoluminescence spectra of surface vanadyl groups. Direct evidence for change of bond strength and electronic structure of metal-oxygen bond upon supporting oxide. Journal of the American Chemical Society. 1983;105(11):3719-3720.
36. Sakthivel P, Murugan R, Asaithambi S, Karuppaiah M, Vijayaprasath G, Rajendran S, et al. Radio frequency power induced changes of structural, morphological, optical and electrical properties of sputtered cadmium oxide thin films. Thin Solid Films. 2018;654:85-92.
37. Liqiang J, Yichun Q, Baiqi W, Shudan L, Baojiang J, Libin Y, et al. Review of photoluminescence performance of nano-sized semiconductor materials and its relationships with photocatalytic activity. Sol Energy Mater Sol Cells. 2006;90(12):1773-1787.
38. Kumari L, Li WZ, Vannoy CH, Leblanc RM, Wang DZ. Vertically aligned and interconnected nickel oxide nanowalls fabricated by hydrothermal route. Cryst Res Technol. 2009;44(5):495-499.
39. Mohseni Meybodi S, Hosseini SA, Rezaee M, Sadrnezhaad SK, Mohammadyani D. Synthesis of wide band gap nanocrystalline NiO powder via a sonochemical method. Ultrason Sonochem. 2012;19(4):841-845.
40. Gnanam S, Rajendran V. Preparation of Cd-doped SnO2 nanoparticles by sol–gel route and their optical properties. J Sol-Gel Sci Technol. 2010;56(2):128-133.
41. Zhang J, Au KH, Zhu ZQ, O'Shea S. Sol–gel preparation of poly(ethylene glycol) doped indium tin oxide thin films for sensing applications. Opt Mater. 2004;26(1):47-55.
42. Sheny DS, Mathew J, Philip D. Phytosynthesis of Au, Ag and Au–Ag bimetallic nanoparticles using aqueous extract and dried leaf of Anacardium occidentale. Spectrochimica Acta Part A: Molecular and Biomolecular Spectroscopy. 2011;79(1):254-262.
43. Lamers RP, Stinnett JW, Muthukrishnan G, Parkinson CL, Cole AM. Evolutionary analyses of Staphylococcus aureus identify genetic relationships between nasal carriage and clinical isolates. PLoS One. 2011;6(1):e16426-e16426.
44. Shakerimoghaddam A, Safardoust-Hojaghan H, Amiri O, Salavati-Niasari M, Khorshidi A, Khaledi A. $Ca_{19}Zn2(PO_4)_{14}$ Nanoparticles: Synthesis, characterization and its effect on the colonization of Streptococcus mutans on tooth surface. J Mol Liq. 2022;350:118507.
45. Erol S, Altoparlak U, Akcay MN, Celebi F, Parlak M. Changes of microbial flora and wound colonization in burned patients. Burns. 2004;30(4):357-361.
46. Wu C, Labrie J, Tremblay YDN, Haine D, Mourez M, Jacques M. Zinc as an agent for the prevention of biofilm formation by pathogenic bacteria. J Appl Microbiol. 2013;115(1):30-40.
47. Janardan S, Suman P, Ragul G, Anjaneyulu U, Shivendu R, Dasgupta N, et al. Assessment on the antibacterial activity of nanosized silica derived from hypercoordinated silicon(iv) precursors. RSC Advances. 2016;6(71):66394-66406.